Available online at www.sciencedirect.com
ScienceDirect
Tetrahedron
Tetrahedron 63 (2007) 3882–3893

Reactions of azulene and guaiazulene with all-*trans*-retinal and *trans*-cinnamaldehyde: comparative studies on spectroscopic, chemical, and electrochemical properties of monocarbenium-ions stabilized by expanded π-electron systems with an azulenyl or 3-guaiazulenyl group

Shin-ichi Takekuma,[a,*] Kazutaka Mizutani,[a] Kanako Inoue,[a] Masaru Nakamura,[a] Masato Sasaki,[a] Toshie Minematsu,[b] Kunihisa Sugimoto[c] and Hideko Takekuma[a]

[a]*Department of Applied Chemistry, Faculty of Science and Engineering, Kinki University, 3-4-1 Kowakae, Higashi-Osaka-shi, Osaka 577-8502, Japan*
[b]*School of Pharmaceutical Sciences, Kinki University, 3-4-1 Kowakae, Higashi-Osaka-shi, Osaka 577-8502, Japan*
[c]*Rigaku Corporation, 3-9-12 Matsubara-cho, Akishima-shi, Tokyo 196-8666, Japan*

Received 26 July 2006; accepted 8 February 2007
Available online 21 February 2007

Abstract—Reaction of azulene (**1**) with all-*trans*-retinal in diethyl ether in the presence of hexafluorophosphoric acid at −10 °C for 1 h in a dark room gives the corresponding monocarbenium-ion compound, (2*E*,4*E*,6*E*,8*E*)-1-azulenyl-3,7-dimethyl-9-(2,6,6-trimethyl-1-cyclohexen-1-yl)-2,4,6,8-nonatetraen-1-ylium hexafluorophosphate (**3**), in 74% isolated yield. The spectroscopic, chemical, and electrochemical properties of **3** compared with those of the previously-documented (2*E*,4*E*,6*E*,8*E*)-1-(3-guaiazulenyl)-3,7-dimethyl-9-(2,6,6-trimethyl-1-cyclohexen-1-yl)-2,4,6,8-nonatetraen-1-ylium hexafluorophosphate (**4**) are reported. Along with the above delocalized monocarbenium-ion compounds **3** and **4**, stabilized by the expanded π-electron systems possessing an azulenyl (or 3-guaiazulenyl) group, an efficient preparation as well as the spectroscopic, chemical, and electrochemical properties of (2*E*)-1-azulenyl-3-phenyl-2-propen-1-ylium and (2*E*)-1-(3-guaiazulenyl)-3-phenyl-2-propen-1-ylium hexafluorophosphates (**5** and **6**) (90 and 96% isolated yields), having a similar partial structure [i.e., the (2*E*)-1-azulenyl-2-propen-1-ylium-ion or (2*E*)-1-(3-guaiazulenyl)-2-propen-1-ylium-ion part] to those of **3** and **4**, is documented. Moreover, the crystal structure of **6**, whose carbenium-ion framework is planar, is shown.
© 2007 Elsevier Ltd. All rights reserved.

1. Introduction

The synthesis, stability, spectroscopic and chemical properties, crystal structures, electrochemical behavior, and, further, theoretical study (e.g., ab initio calculations, DFT, GIAO-NMR, and NICS) of the azulenium-,[1–4] azulenylium-(and azulenylmethylium-)[5–14] ions, and the azulen-1-yl-substituted cations[15–18] have been studied to a considerable extent, and a large number of the results and discussion regarding those cations with delocalized π-electron systems have been well documented. Along with the above investigations, we previously reported a facile preparation and the crystal structures as well as the spectroscopic, chemical, and electrochemical properties of the delocalized mono- and dicarbenium-ions stabilized by the expanded π-electron systems with a 3-guaiazulenyl group.[19–32] During the course of our basic and systematic studies on the 3-guaiazulenyl-substituted carbenium-ions with the characteristic properties of naturally occurring guaiazulene[23,26,33] (**2**), we have recently found (i) that the reaction of **2** with all-*trans*-retinal in methanol in the presence of hexafluorophosphoric acid gave (2*E*,4*E*,6*E*,8*E*)-1-(3-guaiazulenyl)-3,7-dimethyl-9-(2,6,6-trimethyl-1-cyclohexen-1-yl)-2,4,6,8-nonatetraen-1-ylium hexafluorophosphate (**4**), quantitatively;[24] (ii) that the reduction potential of **4** showed that **4** underwent one-electron reduction at −0.24 (E_{pc}, irreversible) V by CV [and −0.19 (E_p) V by DPV] (see Fig. 2), generating the corresponding electrochemically unstable radical species; and have quite recently found (iii) that the crystal structure of (2*E*)-1-(3-guaiazulenyl)-3-phenyl-2-propen-1-ylium hexafluorophosphate (**6**), possessing a similar partial structure [i.e., the (2*E*)-1-(3-guaiazulenyl)-2-propen-1-ylium-ion part] to that of **4**, could be clarified by means of the X-ray diffraction (see Section 4.1.6). In relation to this study, in 1986 Katagiri and his coworkers reported the electrophotographic photoconductors using (2*E*)-1-(3-guaiazulenyl)-3-[4-(dimethylamino)phenyl]-2-

Keywords: All-*trans*-retinal; Azulene; Carbenium-ions; Electrochemical behavior; Guaiazulene; $NaBH_4$-reduction; Spectroscopic properties; *trans*-Cinnamaldehyde; X-ray crystal structure.
* Corresponding author. Tel.: +81 6 6730 5880x4020; fax: +81 6 6727 4301; e-mail: takekuma@apch.kindai.ac.jp

0040–4020/$ - see front matter © 2007 Elsevier Ltd. All rights reserved.
doi:10.1016/j.tet.2007.02.071

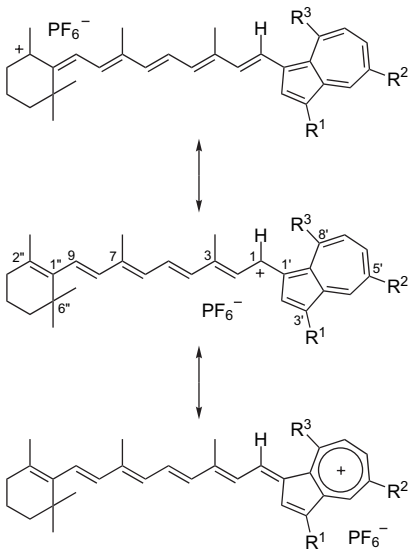

3: $R^1 = R^2 = R^3 = H$
4: $R^1 = R^3 = CH_3$, $R^2 = CH(CH_3)_2$

Chart 1.

propen-1-ylium salts (i.e., BF_4^-, ClO_4^-,[5b,18] Br^-, and I^-),[34] however, nothing has really been documented regarding their accurate spectral data, crystal structures, and other properties. As a series of our basic studies on carbenium-ions stabilized by expanded π-electron systems with an azulenyl (or 3-guaiazulenyl) group, our interest has quite recently been focused on the title chemistry; namely, comparative studies on a facile preparation, molecular structures, and properties of (2*E*,4*E*,6*E*,8*E*)-1-azulenyl-3,7-dimethyl-9-(2,6,6-trimethyl-1-cyclohexen-1-yl)-2,4,6,8-nonatetraen-1-ylium hexafluorophosphate (**3**), **4**, and (2*E*)-1-azulenyl-3-phenyl-2-propen-1-ylium and (2*E*)-1-(3-guaiazulenyl)-3-phenyl-2-propen-1-ylium hexafluorophosphates (**5** and **6**) with the resonance forms illustrated in Charts 1 and 2. We now wish to report the detailed studies on an efficient preparation as well as the spectroscopic, chemical, and electrochemical properties of **3**–**6** with a view to a comparative study along with the crystal structure of **6**.

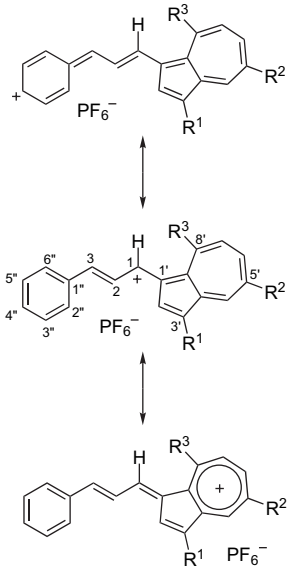

5: $R^1 = R^2 = R^3 = H$
6: $R^1 = R^3 = CH_3$, $R^2 = CH(CH_3)_2$

Chart 2.

2. Results and discussion

2.1. Preparation and spectroscopic and chemical properties of 3

The target compound **3** was prepared according to the procedure shown in Section 4.1.1, whose molecular structure was established on the basis of elemental analysis and spectroscopic data [UV–vis, IR, exact FABMS, and ^1H and ^{13}C NMR including 2D NMR (i.e., H–H COSY, HMQC, and HMBC)].

Compound **3**[35] (74% isolated yield) was a dark-blue powder, mp >135 °C (decomp.). A comparative study on the UV–vis [λ_{max} (CH_3CN), nm] spectrum of **3** with those of azulene[36] and **4**[24] showed (i) that, similarly as in the case of **4**, no characteristic UV–vis absorption bands based on the azulenyl group were observed, indicating the formation of the molecular structure **3** with a delocalized π-electron system between the azulenyl group and the (2*E*,4*E*,6*E*,8*E*)-3,7-dimethyl-9-(2,6,6-trimethyl-1-cyclohexen-1-yl)-2,4,6,8-nonatetraen-1-ylium-ion part; and (ii) that, although the spectral pattern of the characteristic UV–vis absorption bands for **3** resembled that of **4**, the longest absorption wavelength of **3** (λ_{max} 683 nm, log ε=4.79) revealed a bathochromic shift (Δ 28 nm) in comparison with that of **4** (λ_{max} 655 nm, log ε=4.82), owing to a difference in HOMO–LUMO gap (Δ eV) (see Fig. 1). The IR (KBr) spectrum showed two specific bands based on the counter anion (PF_6^-) at ν_{max} 841 and 559 cm^{-1}, whose wavenumbers coincided with those of **4** (ν_{max} 837 and 555 cm^{-1}).[24] The molecular formula $C_{30}H_{35}$ ($[M-PF_6]^+$) was determined by the exact FABMS spectrum using 3-nitrobenzyl alcohol as a matrix reagent. An elemental analysis confirmed the molecular formula $C_{30}H_{35}F_6P$. The 700 MHz ^1H NMR (CD_3CN) spectrum showed signals based on the azulenyl group with the resonance form of

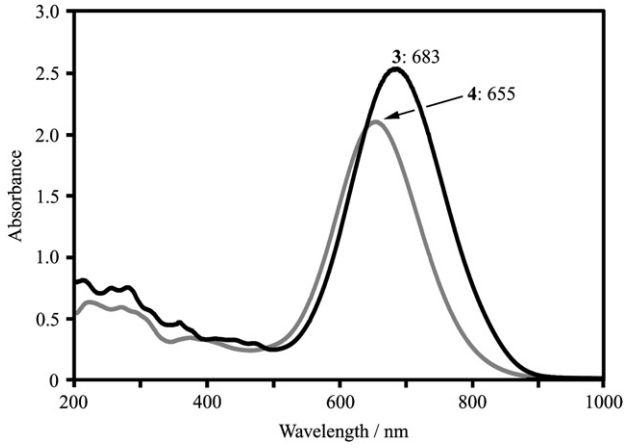

Figure 1. The UV–vis spectra of **3** and **4** in CH_3CN. Concentrations: **3**, 0.022 g/L (40.7 μmol/L); **4**, 0.020 g/L (31.8 μmol/L). Length of the cell: 1 cm each.

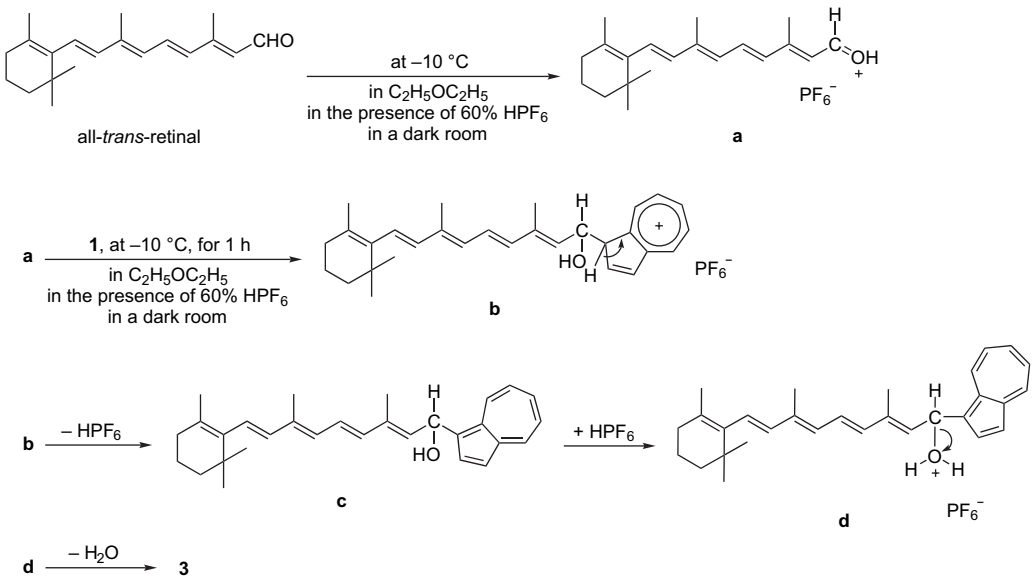

Scheme 1. A plausible reaction pathway for the formation of **3** yielded by the reaction of **1** with all-*trans*-retinal in diethyl ether in the presence of hexafluorophosphoric acid (60% aqueous solution) at −10 °C for 1 h in a dark room.

the azulenylium-ion, and revealed signals based on the (2*E*,4*E*,6*E*,8*E*)-3,7-dimethyl-9-(2,6,6-trimethyl-1-cyclohexen-1-yl)-2,4,6,8-nonatetraen-1-ylium-ion part with a delocalized π-electron system, whose signals (δ and *J* values) were carefully assigned using the H–H COSY technique and the computer-assisted simulation analysis (see Section 4.1.1). The 176 MHz ^{13}C NMR (CD_3CN) spectrum exhibited 27 carbon signals assigned by the HMQC and HMBC techniques (see Section 4.1.1). Thus, the elemental analysis and these spectroscopic data for **3** led to the molecular structure (2*E*,4*E*,6*E*,8*E*)-1-azulenyl-3,7-dimethyl-9-(2,6,6-trimethyl-1-cyclohexen-1-yl)-2,4,6,8-nonatetraen-1-ylium hexafluorophosphate with the resonance forms illustrated in Chart 1.

From the molecular structure of the resulting product **3**, a plausible reaction pathway for the formation of **3** can be inferred as illustrated in Scheme 1; namely, the generated protonated-compound **a** is gradually converted to **3** presumably via the azulenylium-ion **b**, the secondary alcohol form **c** and the dehydration from the oxonium-ion **d**.

The chemical shifts (δ, ppm) for the proton and carbon signals of **3** and **4**[24] with a view to a comparative study are shown in Tables 1–4. As the results, it was found (i) that the proton signal of the H-1 (8.56) of **3** showed an up-field shift in comparison with that of **4** (H-1: 8.68), however, the proton signals of the H-2′ (8.30), H-4′ (8.65), H-5 (7.60), and H-9 (6.71) of **3** revealed down-field shifts in comparison with those of **4** (H-2′: 8.12, H-4′: 8.50, H-5: 7.49, and H-9: 6.59) (see Tables 1 and 2); and (ii) that, although the carbon signal of the C-1 (146.1) of **3** coincided with that of **4** (145.6), the carbon signals of the C-1′ (136.4), C-3a′ (151.8), and C-7′ (139.6) of **3** showed up-field shifts in comparison with those of **4** (C-1′: 137.8, C-3a′: 158.0, and C-7′: 147.1), and the carbon signals of the C-2′ (140.0), C-4′ (143.0), C-6′ (146.3), C-8a′ (157.5), C-3 (167.3), C-5 (142.8), C-7 (151.4), C-9 (135.6), and C-2″ (135.3) of **3** revealed down-field shifts in comparison with those of **4** (C-2′: 139.0, C-4′: 139.2, C-6′: 143.5, C-8a′: 150.7, C-3: 161.1, C-5: 138.5, C-7: 147.0, C-9: 133.1, and C-2″: 133.2) (see Tables 3 and 4). Thus, an apparent difference between the

Table 1. The ^{1}H NMR chemical shifts (δ, ppm) for the azulen-1-yl groups of **3** and **4**

Compound	H-2′	H-3′	H-4′	H-5′	H-6′	H-7′	H-8′
3	8.30	7.66	8.65	8.12	8.28	8.19	9.12
4[a]	8.12	—	8.50	—	8.23	8.25	—
Difference[b]	+0.18	—	+0.15	—	+0.05	−0.06	—

[a] For a comparative purpose, the numbering scheme of the 3-guaiazulenyl group of **4** was changed to that of the 3,8-dimethyl-5-isopropylazulen-1-yl group (see Charts 1 and 2).
[b] The difference between the chemical shifts of **3** and those of **4**.

Table 2. The ^{1}H NMR chemical shifts (δ, ppm) for the (2*E*,4*E*,6*E*,8*E*)-2,4,6,8-nonatetraen-1-ylium-ion parts of **3** and **4**

Compound	H-1	H-2	H-4	H-5	H-6	H-8	H-9
3	8.56	7.38	6.70	7.60	6.42	6.38	6.71
4	8.68	7.34	6.74	7.49	6.44	6.35	6.59
Difference[a]	−0.12	+0.04	−0.04	+0.11	−0.02	+0.03	+0.12

[a] The difference between the chemical shifts of **3** and those of **4**.

Table 3. The ^{13}C NMR chemical shifts (δ, ppm) for the azulen-1-yl groups of **3** and **4**

Compound	C-1′	C-2′	C-3′	C-3a′	C-4′	C-5′	C-6′	C-7′	C-8′	C-8a′
3	136.4	140.0	132.6	151.8	143.0	141.3	146.3	139.6	140.0	157.5
4[a]	137.8	139.0	142.2[c]	158.0	139.2	166.1[d]	143.5	147.1	155.8[c]	150.7
Difference[b]	−1.4	+1.0	−9.6	−6.2	+3.8	−24.8	+2.8	−7.5	−15.8	+6.8

[a] For a comparative purpose, the numbering scheme of the 3-guaiazulenyl group of **4** was changed to that of the 3,8-dimethyl-5-isopropylazulen-1-yl group (see Charts 1 and 2).
[b] The difference between the chemical shifts of **3** and those of **4**.
[c] The methyl-substituted carbon.
[d] The isopropyl-substituted carbon.

Table 4. The selected ^{13}C NMR chemical shifts (δ, ppm) for the (2*E*,4*E*,6*E*,8*E*)-9-(1-cyclohexen-1-yl)-2,4,6,8-nonatetraen-1-ylium-ion parts of **3** and **4**

Compound	C-1	C-2	C-3	C-4	C-5	C-6	C-7	C-8	C-9	C-1″	C-2″
3	146.1	131.7	167.3	137.7	142.8	132.8	151.4	137.7	135.6	138.9	135.3
4	145.6	131.2	161.1	137.4	138.5	132.1	147.0	137.9	133.1	138.7	133.2
Difference[a]	+0.5	+0.5	+6.2	+0.3	+4.3	+0.7	+4.4	−0.2	+2.5	+0.2	+2.1

[a] The difference between the chemical shifts of **3** and those of **4**.

chemical shifts for the proton and carbon signals of **3** and those of **4** was observed, owing to a difference in azulenyl group. Furthermore, although the reduction of **3** with $NaBH_4$ in methylene-d_2 chloride at −10 °C for 20 min in a dark room gave several chromatographically inseparable products, suggesting the formation of different kinds of H^- reduction products, simultaneously, the reduction of **4** under the same reaction conditions as for **3** afforded (2*E*,4*E*,6*E*,8*E*)-1-(3-guaiazulenyl)-3,7-dimethyl-9-(2,6,6-trimethyl-1-cyclohexen-1-yl)-2,4,6,8-nonatetraene (**7**), quantitatively (see Section 4.1.2), in which a hydride-ion was attached to the C-1 position of **4**, selectively (see Chart 3). Thus, an apparent difference between the $NaBH_4$-reduction behavior of **3** and that of **4** was observed. From a comparative study on the chemical shifts for the proton and carbon signals of **4** with those of **7**, it was found that all the proton signals of **4** showed larger down-field shifts and the carbon signals of the C-1′, 3′, 3a′, 4′–8′, 8a′, 1, 3, 5, 7, 9, and 2″ positions of **4** revealed larger down-field shifts, suggesting the formation of **4** with a delocalized π-electron system and, further, the same result could be inferred for **3** (see Chart 1).

2.2. The electrochemical behavior of 3 and 4

The electrochemical behavior of **3** was measured by means of the CV and DPV (potential/V vs SCE) in CH_3CN containing 0.1 M [*n*-Bu_4N]PF_6 as a supporting electrolyte under the same electrochemical measurement conditions as for **4**.[24] From a comparative study on the reduction potential of **3** with that of **4**, it can be inferred that **3** and **4** undergo one-electron reduction at the potentials of −0.08 (E_{pc}, irreversible) V by CV [and −0.05 (E_p) V by DPV] for **3** and of −0.24 (E_{pc} irreversible) V by CV [and −0.19 (E_p) V by DPV] for **4** as shown in Figure 2, generating the corresponding electrochemically unstable radical species. Thus, **3** is more susceptible to reduction as compared with **4**. In relation to the difference between the electrochemical behavior of the azulenyl-substituted π-electron system and that of the 3-guaiazulenyl-substituted π-electron system, we recently reported that 2-azulenyl-1,1-bis(4-methoxyphenyl)ethylene (**8**) [−1.53 ($E_{1/2}$) V by CV and −1.51 (E_p) V by DPV] was more susceptible to one-electron reduction than 2-(3-guaiazulenyl)-1,1-bis(4-methoxyphenyl)ethylene (**9**) [−1.73 ($E_{1/2}$) V by CV and −1.70 (E_p) V by DPV] (see Chart 4), owing to a difference in electron affinity [corresponding to π-LUMO (eV)] based on the expanded π-electron system possessing an azulenyl (or 3-guaiazulenyl) group,[37] generating an anion-radical species.[26] Moreover, in the previous papers,[23,27] we reported the electrochemical behavior of several (3-guaiazulenyl)phenylmethylium-ions and submitted a plausible electron transfer mechanism of those monocarbenium-ions based on the CV and DPV data and, further, clarified that the generated radical species were rapidly converted to the radical homo-coupling products, respectively. The molecular structures of the products from the electrochemical reductions of **3** and **4** under the above CV and DPV measurement conditions are currently under intensive investigation.

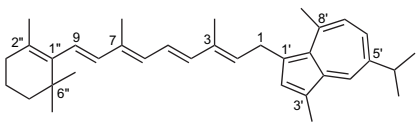

7

Chart 3.

2.3. Preparation and spectroscopic and chemical properties of 5 and 6

The target compounds **5** and **6** were prepared according to the procedures shown in Sections 4.1.3 and 4.1.4. The molecular structures of **5** and **6** were established on the basis of elemental analysis and similar spectroscopic analyses to those of **3** (see Sections 2.1 and 4.1.1).

Compound **5** (90% isolated yield) was a dark-red powder, mp >120 °C (decomp.). Similarly, as in the cases of **3** and **4**, the characteristic UV–vis [λ_{max} (CH_3CN), nm] absorption bands based on **1**[36] were not observed, indicating the formation of the molecular structure **5** with a delocalized π-electron system between the azulenyl group and the (2*E*)-3-phenyl-2-propen-1-ylium-ion part, and the longest visible absorption wavelength appeared at λ_{max} 500 nm (log ε=4.55) (see Fig. 3). The IR (KBr) spectrum showed two specific bands based on the counter anion (PF_6^-) at

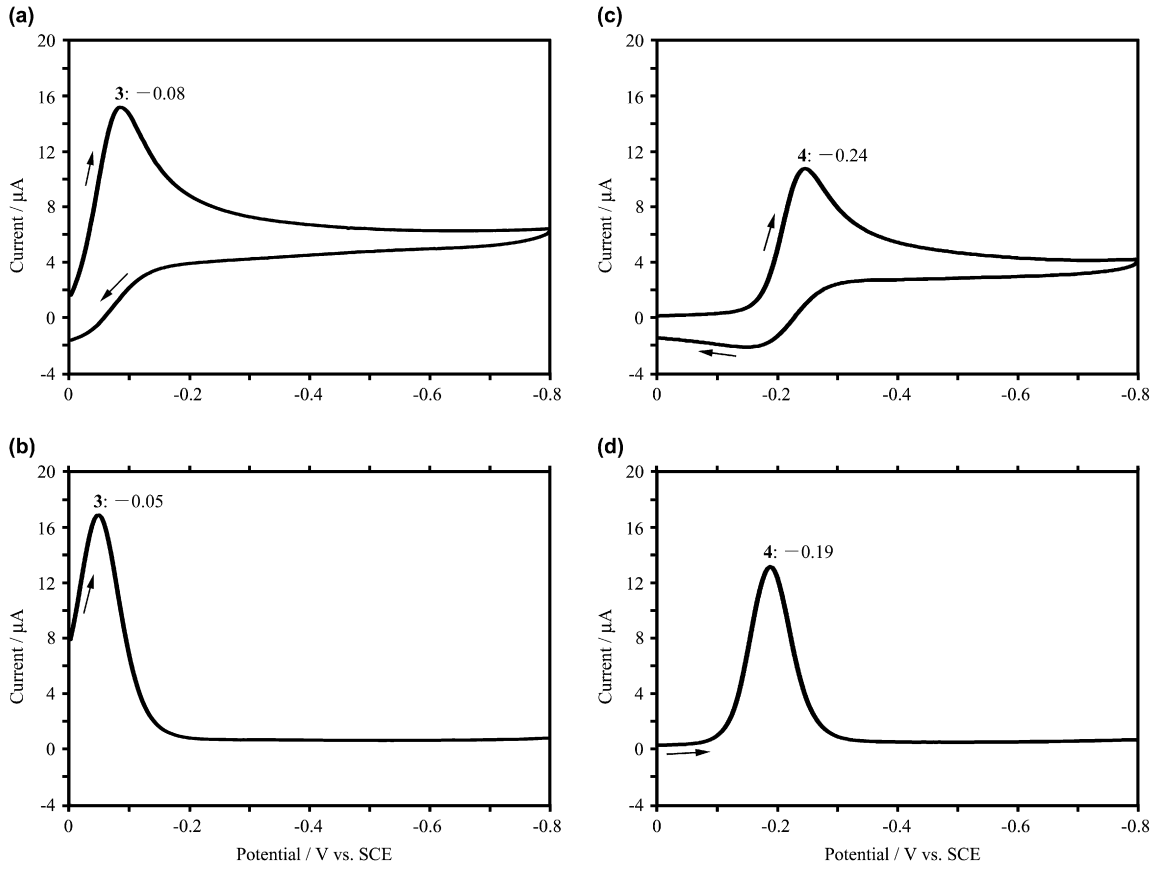

Figure 2. Cyclic (a,c) and differential pulse (b,d) voltammograms of **3** (3.0 mg, 5.5 μmol) and **4** (3.0 mg, 4.9 μmol) in 0.1 M [*n*-Bu_4N]PF_6, CH_3CN (10 mL) at a glassy carbon (ID: 3 mm) and a platinum wire served as the working and auxiliary electrodes, scan rates 100 mV/s at 25 °C under argon, respectively. For comparative purposes, the oxidation potential using ferrocene as a standard material showed +0.42 (E_p) V by DPV and +0.40 ($E_{1/2}$) V by CV under the same electrochemical measurement conditions as for **3** and **4**.

ν_{max} 837 and 556 cm^{-1}, whose wavenumbers coincided with those of **3** (ν_{max} 841 and 559 cm^{-1}) and **4** (ν_{max} 837 and 555 cm^{-1}). The molecular formula $C_{19}H_{15}$ ($[M-PF_6]^+$) was determined by the exact FABMS spectrum using 3-nitrobenzyl alcohol as a matrix reagent. The 500 MHz ^1H NMR (CD_3CN) spectrum showed signals based on the azulenyl group with the resonance form of the azulenylium-ion, and revealed signals based on the (2*E*)-3-phenyl-2-propen-1-ylium-ion part with a delocalized π-electron system, whose signals (δ and J values) were carefully assigned using the H–H COSY technique and the computer-assisted simulation analysis (see Section 4.1.3). The 125 MHz ^{13}C NMR (CD_3CN) spectrum exhibited 17 carbon signals assigned by the HMQC and HMBC techniques (see Section 4.1.3). Thus, these spectroscopic data for **5** led to the molecular structure (2*E*)-1-azulenyl-3-phenyl-2-propen-1-ylium hexafluorophosphate with the resonance forms illustrated in Chart 2.

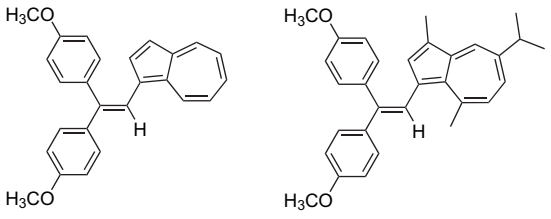

8 **9**

Chart 4.

Compound **6** (96% isolated yield) was dark-red blocks, mp >151 °C [decomp., determined by the thermal analyses (TGA[38] and DTA)]. A comparative study on the UV–vis [λ_{max} (CH_3CN), nm] spectrum of **6** with that of **5** showed (i) that, similarly as in the case of **5**, no characteristic UV–vis absorption bands based on guaiazulene[39] were observed, indicating the formation of the molecular structure **6** with a delocalized π-electron system between the 3-guaiazulenyl group and the (2*E*)-3-phenyl-2-propen-1-ylium-ion part; (ii)

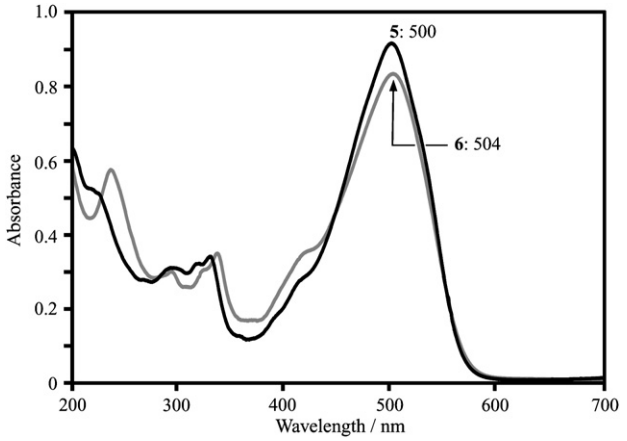

Figure 3. The UV–vis spectra of **5** and **6** in CH_3CN. Concentrations: **5**, 0.010 g/L (25.8 μmol/L); **6**, 0.011 g/L (24.0 μmol/L). Length of the Cell: 1 cm each.

that the spectral pattern of the characteristic UV–vis absorption bands for **6** resembled that of **5**; and (iii) that, although the longest absorption wavelength of **3** (λ_{max} 683 nm, log ε= 4.79) revealed a bathochromic shift (Δ 28 nm) in comparison with that of **4** (λ_{max} 655 nm, log ε=4.82) (see Fig. 1), the longest absorption wavelength of **6** (λ_{max} 504 nm, log ε= 4.54) coincided with that of **5** (λ_{max} 500 nm, log ε=4.55) (see Fig. 3), owing to a difference in HOMO–LUMO gap (Δ eV).[40] The IR (KBr) spectrum showed two specific bands based on the counter anion (PF_6^-) at ν_{max} 837 and 559 cm^{-1}, whose wavenumbers coincided with those of **5** (ν_{max} 837 and 556 cm^{-1}). The molecular formula $C_{24}H_{25}$ ($[M-PF_6]^+$) was determined by the exact FABMS spectrum using 3-nitrobenzyl alcohol as a matrix reagent. An elemental analysis confirmed the molecular formula $C_{24}H_{25.25}F_6O_{0.125}P$ (i.e., $C_{24}H_{25}F_6P+1/8H_2O$), whose result was supported by the TGA.[38] The 500 MHz ^1H NMR (CD_3CN) spectrum showed signals based on the 3-guaiazulenyl group with the resonance form of the 3-guaiazulenylium-ion, and revealed signals based on the (2*E*)-3-phenyl-2-propen-1-ylium-ion part with a delocalized π-electron system, whose signals were carefully assigned using the H–H COSY technique and the computer-assisted simulation analysis (see Section 4.1.4). The 125 MHz ^{13}C NMR (CD_3CN) spectrum exhibited 21 carbon signals assigned by the HMQC and HMBC techniques (see Section 4.1.4). Thus, the elemental analysis and these spectroscopic data for **6** led to the molecular structure (2*E*)-1-(3-guaiazulenyl)-3-phenyl-2-propen-1-ylium hexafluorophosphate with the resonance forms illustrated in Chart 2. Similarly, as in the cases of **3** and **4**, although the reduction of **5** with $NaBH_4$ in methylene-d_2 chloride at 25 °C for 20 min gave several chromatographically inseparable products, suggesting the formation of different kinds of H^- reduction products, simultaneously, the reduction of **6** under the same reaction conditions as for **5** afforded (2*E*)-1-(3-guaiazulenyl)-3-phenyl-2-propene (**10**), quantitatively (see Section 4.1.5), in which a hydride-ion was attached to the C-1 position of **6**, selectively (see Chart 5). Thus, an apparent difference between the $NaBH_4$-reduction behavior of **5** and that of **6** was observed. From a comparative study on the chemical shifts for the proton and carbon signals of **6** with those of **10**, it was found that all the proton signals of **6** showed larger down-field shifts and the carbon signals of the C-1′, 3′, 3a′, 4′–8′, 8a′, 1, 3, 2″, 4″, and 6″ positions

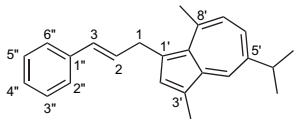

10

Chart 5.

of **6** revealed larger down-field shifts, suggesting the formation of **6** with a delocalized π-electron system and, further, the same result could be inferred for **5** (see Chart 2).

Table 6. The ^1H NMR chemical shifts (δ, ppm) for the (2*E*)-3-phenyl-2-propen-1-ylium-ion parts of **5** and **6**

Compound	H-1	H-2	H-3	H-2″,6″	H-3″,5″	H-4″
5	8.58	8.08	7.83	7.83	7.50	7.53
6	8.45	7.87	7.65	7.72	7.42	7.43
Difference[a]	+0.13	+0.21	+0.18	+0.11	+0.08	+0.10

[a] The difference between the chemical shifts of **5** and those of **6**.

The chemical shifts (δ, ppm) for the proton and carbon signals of **5** and **6** with a view to a comparative study are shown in Tables 5–8. As the results, it was found (i) that all the proton signals of **5** revealed down-field shifts in comparison with those of **6** (see Tables 5 and 6); and (ii) that the carbon signals of the C-3a′ (154.6) and C-7′ (143.7) of **5** showed up-field shifts in comparison with those of **6** (C-3a′: 160.7 and C-7′: 149.5), however, the carbon signals of the C-1′ (139.0), C-2′ (141.5), C-4′ (144.3), C-6′ (147.8), C-8a′ (161.4), C-1 (152.1), C-3 (156.7), C-2″,6″ (130.9), and C-4″ (133.8) of **5** revealed down-field shifts in comparison with those of **6** (C-1′: 136.7, C-2′: 139.7, C-4′: 139.7, C-6′: 144.5, C-8a′: 152.1, C-1: 150.8, C-3: 152.9, C-2″,6″: 130.1, and C-4″: 132.7) (see Tables 7 and 8). Similarly, as in the cases of **3** and **4**, an apparent difference between the chemical shifts for the proton and carbon signals of **5** and those of **6** was observed, owing to a difference in azulenyl group.

2.4. X-ray crystal structure of 6

Although an X-ray crystallographic analysis of **3**–**5** has not yet been achieved, because it was very difficult to obtain a single crystal suitable for this purpose, the crystal structure of **6** with a 1/8 M amount of H_2O molecule[38] (see Section 4.1.4) has been determined by means of the X-ray diffraction (see Section 4.1.6). In the course of refinement, the carbon atoms based on the isopropyl group for **6** were found to be disordered over two sites of 70:30 occupancy. Therefore, those atoms in the occupancy ratio 70:30 were refined. The only ORTEP drawing of **6**, which noted the above disorder, indicating the molecular structure (2*E*)-1-(3-guaiazulenyl)-3-phenyl-2-propen-1-ylium hexafluorophosphate is shown in Figure 4 together with the selected bond lengths. As the result, the structural parameters of **6** revealed (i) that the carbenium-ion framework was planar. Thus, the formation of a delocalized π-electron system between the 3-guaiazulenyl group and the (2*E*)-3-phenyl-2-propen-1-ylium-ion part is possible; (ii) that, similarly as in the case of (3-guaiazulenyl)phenylmethylium hexafluorophosphate[22,23] (**11**), the 3-guaiazulenylmethylium-ion part

Table 5. The ^1H NMR chemical shifts (δ, ppm) for the azulen-1-yl groups of **5** and **6**

Compound	H-2′	H-3′	H-4′	H-5′	H-6′	H-7′	H-8′
5	8.50	7.82	8.90	8.51	8.57	8.55	9.25
6[a]	8.19	—	8.51	—	8.32	8.37	—
Difference[b]	+0.31	—	+0.39	—	+0.25	+0.18	—

[a] For a comparative purpose, the numbering scheme of the 3-guaiazulenyl group of **6** was changed to that of the 3,8-dimethyl-5-isopropylazulen-1-yl group (see Charts 1 and 2).
[b] The difference between the chemical shifts of **5** and those of **6**.

Table 7. The ^{13}C NMR chemical shifts (δ, ppm) for the azulen-1-yl groups of **5** and **6**

Compound	C-1′	C-2′	C-3′	C-3a′	C-4′	C-5′	C-6′	C-7′	C-8′	C-8a′
5	139.0	141.5	135.4	154.6	144.3	145.7	147.8	143.7	141.0	161.4
6[a]	136.7	139.7	143.7[c]	160.7	139.7	169.6[d]	144.5	149.5	157.2[c]	152.1
Difference[b]	+2.3	+1.8	−8.3	−6.1	+4.6	−23.9	+3.3	−5.8	−16.2	+9.3

[a] For a comparative purpose, the numbering scheme of the 3-guaiazulenyl group of **6** was changed to that of the 3,8-dimethyl-5-isopropylazulen-1-yl group (see Charts 1 and 2).
[b] The difference between the chemical shifts of **5** and those of **6**.
[c] The methyl-substituted carbon.
[d] The isopropyl-substituted carbon.

Table 8. The ^{13}C NMR chemical shifts (δ, ppm) for the (2*E*)-3-phenyl-2-propen-1-ylium-ion parts of **5** and **6**

Compound	C-1	C-2	C-3	C-1″	C-2″,6″	C-3″,5″	C-4″
5	152.1	127.4	156.7	136.4	130.9	130.4	133.8
6	150.8	127.6	152.9	136.7	130.1	130.2	132.7
Difference[a]	+1.3	−0.2	+3.8	−0.3	+0.8	+0.2	+1.1

[a] The difference between the chemical shifts of **5** and those of **6**.

clearly underwent bond alternation between the single and double bonds; (iii) that the (2*E*)-3-phenyl-2-propen-1-ylium-ion part also clearly underwent bond alternation between the single and double bonds; (iv) that the average C–C bond length of the seven-membered ring of the 3-guaiazulenyl group (1.401 Å) coincided with that of **11** (1.401 Å), whose bond length was slightly shorter than that of the parent azulene (1.412 Å),[41] and was longer than those of the azulenium-ions (1.38 Å);[2,3] (v) that the C–C bond lengths of the five-membered ring of the 3-guaiazulenyl group appreciably varied between 1.358 and 1.475 Å; in particular, the C2′–C3′ bond length (1.358 Å) was characteristically shorter than the average C–C bond length for the five-membered ring (1.434 Å), which coincided with the C–C bond lengths observed for the five-membered ring of **11**; (vi) that the C1′–C1 bond length (1.368 Å) was also characteristically shorter than the C1–C2 bond length (1.432 Å); (vii) that the C–C bond length for the vinyl (–CH═CH–) part of **6** (1.342 Å) coincided with that of 4-[2-(*E*)-azulenylethenyl]-*N*-methylpyridinium trifluoromethanesulfonate (**12**) (1.344 Å),[15] and was slightly longer than those of (*E*)-1,2-di(3-guaiazulenyl)ethylene (**13**) (1.32 Å)[26] and *trans*-stilbene (**14**) (1.326 Å);[42] and (viii) that the average C–C bond length for the benzene ring (1.388 Å) coincided with those of the benzene rings of **11** (1.387 Å) and **14** (1.386 Å each). From a comparative study on the detailed spectroscopic properties of **3** (see Section 4.1.1), **4**,[24] and **5** (see Section 4.1.3) with those of **6** (see Section 4.1.4) along with the crystal structures of **6**, **12**, **13**, and *N*-methyl-*N*-phenylretinal iminium perchlorate[43] (**15**), it is presumed (i) that the crystal structure of **5** assumes similar conformation to that of **6**;[44] (ii) that the conformations of the (2*E*,4*E*,6*E*,8*E*)-3,7-dimethyl-9-(2,6,6-trimethyl-1-cyclohexen-1-yl)-2,4,6,8-nonatetraen-1-ylium-ion parts of both **3** and **4** (see Chart 1) are similar to that of the retinal iminium-ion part of **15** (see Chart 6);[44] and

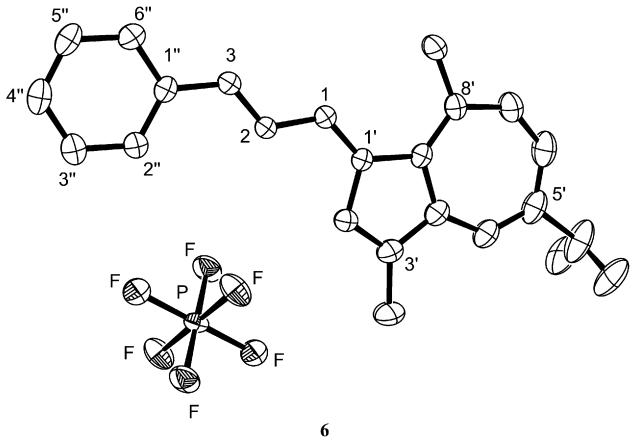

Figure 4. The ORTEP drawing with the numbering scheme (30% probability thermal ellipsoids) of **6**; the H_2O molecule is omitted for reasons of clarity. The selected C–C bond lengths (Å) of **6** are as follows: C1′–C2′, 1.452(4); C2′–C3′, 1.358(5); C3′–C3a′, 1.446(6); C3a′–C4′, 1.396(5); C4′–C5′, 1.372(7); C5′–C6′, 1.412(8); C6′–C7′, 1.373(6); C7′–C8′, 1.419(6); C8′–C8a′, 1.396(5); C8a′–C1′, 1.475(4); C3a′–C8a′, 1.441(4); C1′–C1, 1.368(4); C1–C2, 1.432(4); C2–C3, 1.342(4); C3–C1″, 1.460(5); C1″–C2″, 1.395(5); C2″–C3″, 1.384(5); C3″–C4″, 1.383(5); C4″–C5″, 1.376(7); C5″–C6″, 1.393(6); and C6″–C1″, 1.399(4).

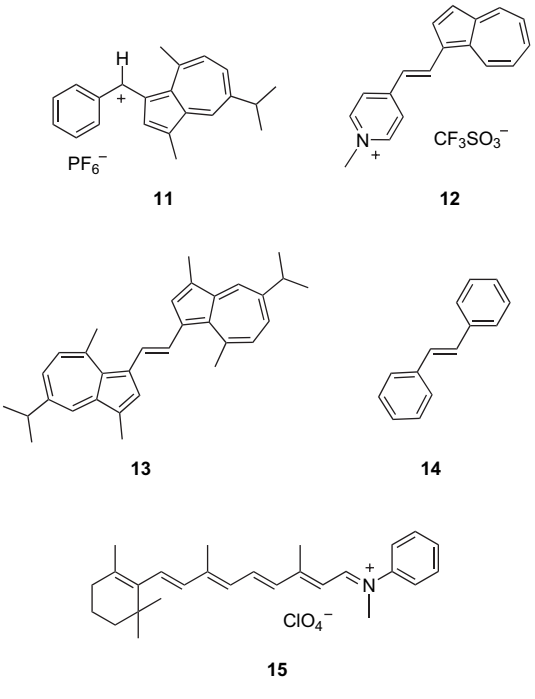

Chart 6.

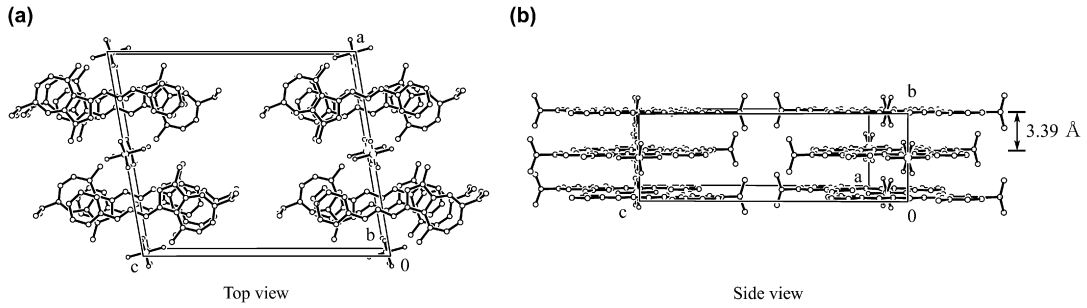

Figure 5. The two different [top (a) and side (b)] views for the packing (molecular) structure of **6**; hydrogen atoms are omitted for reasons of clarity.

(iii) that both the (2*E*,4*E*,6*E*,8*E*)-1-azulenyl-2,4,6,8-nonatetraen-1-ylium-ion framework of **3** and the (2*E*,4*E*,6*E*,8*E*)-1-(3-guaiazulenyl)-2,4,6,8-nonatetraen-1-ylium-ion framework of **4** are planar.[44]

Along with the crystal structure of **6**, the two different (top and side) views for the packing (molecular) structure of **6** revealed that this molecule formed a π-stacking structure in the single crystal, and that the average inter-plane distance between the molecules [i.e., the 3-guaiazulenyl plane of a molecule and the (2*E*)-3-phenyl-2-propen-1-ylium-ion plane of another molecule], which were overlapped so that those dipole moments might be negated mutually, was 3.39 Å (see Fig. 5).

2.5. The electrochemical behavior of 5 and 6

The electrochemical behavior of **5** and **6** was measured by means of the CV and DPV (potential/V vs SCE) in CH_3CN containing 0.1 M [*n*-Bu_4N]PF_6 as a supporting electrolyte under the same electrochemical measurement conditions as for **3** and **4**[24] (see Fig. 2). From a comparative study on the reduction potential of **5** with that of **6**, it can be inferred that **5** and **6** undergo one-electron reduction at the potentials of −0.08 (E_{pc}, irreversible) V by CV [and −0.01 (E_p) V by DPV] for **5**, whose reduction potential coincided with that of **3**, and of −0.23 (E_{pc} irreversible) V by CV [and −0.16 (E_p) V by DPV] for **6**, whose reduction potential coincided with that of **4**, as shown in Figure 6, generating the

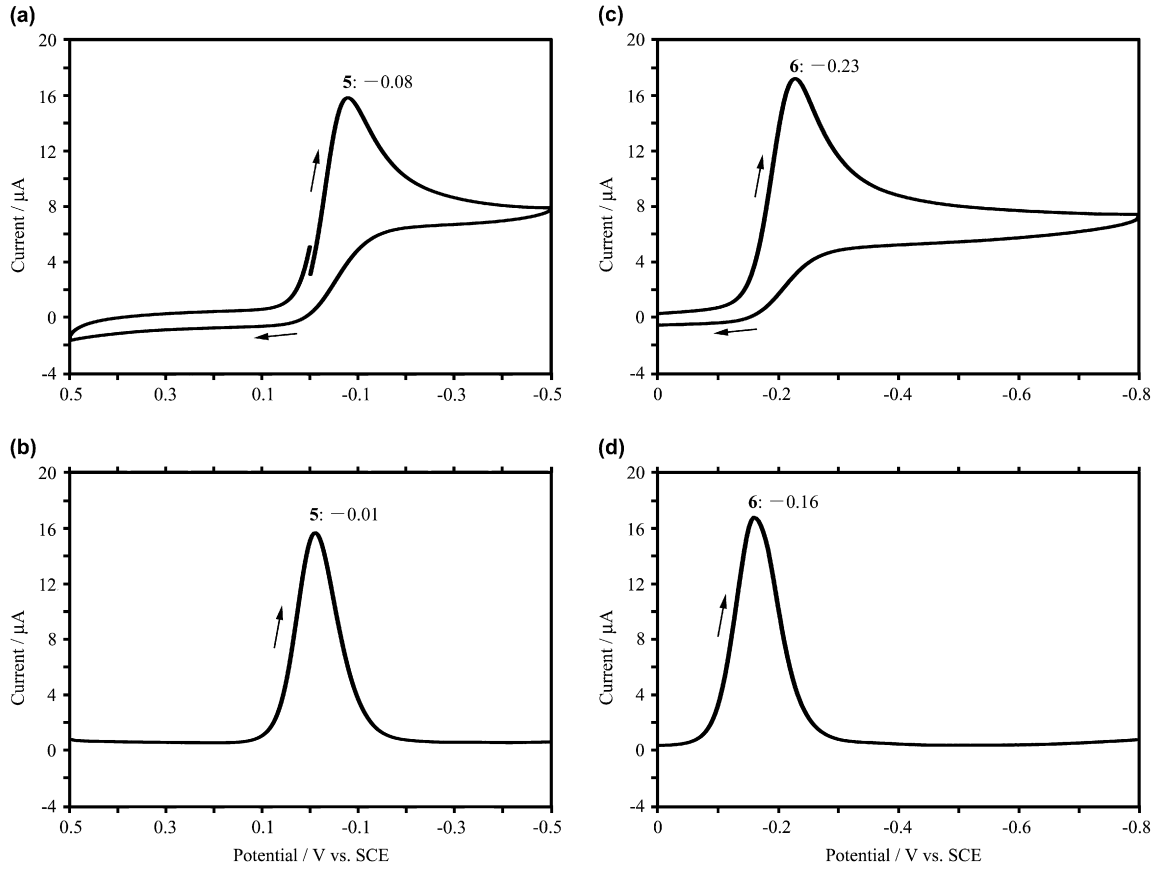

Figure 6. Cyclic (a,c) and differential pulse (b,d) voltammograms of **5** (3.0 mg, 7.7 μmol) and **6** (3.0 mg, 6.5 μmol) in 0.1 M [*n*-Bu_4N]PF_6, CH_3CN (10 mL) under the same electrochemical measurement conditions as for **3** and **4** (see Fig. 2).

corresponding electrochemically unstable radical species. Similarly, as in the case of a comparative study on the reduction potential of **3** with that of **4** (see Section 2.2), **5** is more susceptible to one-electron reduction as compared with **6**, owing to a difference in electron affinity based on the carbenium-ion stabilized by the expanded π-electron system possessing an azulenyl (or 3-guaiazulenyl) group. The molecular structures of the products from the electrochemical reductions of **5** and **6** under the above CV and DPV measurement conditions are currently under intensive investigation.

3. Conclusion

We have reported the following six points in this paper: (i) the reaction of azulene (**1**) with all-*trans*-retinal in diethyl ether in the presence of hexafluorophosphoric acid at −10 °C for 1 h in a dark room gave (2*E*,4*E*,6*E*,8*E*)-1-azulenyl-3,7-dimethyl-9-(2,6,6-trimethyl-1-cyclohexen-1-yl)-2,4,6,8-nonatetraen-1-ylium hexafluorophosphate (**3**) in 74% isolated yield; (ii) the detailed comparative studies on the spectroscopic and electrochemical properties of **3** with those of the previously-documented (2*E*,4*E*,6*E*,8*E*)-1-(3-guaiazulenyl)-3,7-dimethyl-9-(2,6,6-trimethyl-1-cyclohexen-1-yl)-2,4,6,8-nonatetraen-1-ylium hexafluorophosphate (**4**) were reported; (iii) along with the above monocarbenium-ion compounds **3** and **4** stabilized by the expanded π-electron systems possessing an azulenyl (or 3-guaiazulenyl) group, an efficient preparation as well as the spectroscopic and electrochemical properties of (2*E*)-1-azulenyl-3-phenyl-2-propen-1-ylium and (2*E*)-1-(3-guaiazulenyl)-3-phenyl-2-propen-1-ylium hexafluorophosphates (**5** and **6**) (90 and 96% isolated yields), having a similar partial structure [i.e., the (2*E*)-1-azulenyl-2-propen-1-ylium-ion or (2*E*)-1-(3-guaiazulenyl)-2-propen-1-ylium-ion part] to those of **3** and **4**, was documented; (iv) although the reductions of **3** (and **5**) with $NaBH_4$ in methylene-d_2 chloride at −10 °C for 20 min in a dark room (and at 25 °C for 20 min) gave several chromatographically inseparable products, suggesting the formation of different kinds of H^- reduction products, simultaneously, the reductions of **4** (and **6**) under the same reaction conditions as for **3** (and **5**) afforded (2*E*,4*E*,6*E*,8*E*)-1-(3-guaiazulenyl)-3,7-dimethyl-9-(2,6,6-trimethyl-1-cyclohexen-1-yl)-2,4,6,8-nonatetraene (**7**) from **4** and (2*E*)-1-(3-guaiazulenyl)-3-phenyl-2-propene (**10**) from **6**, quantitatively, in which a hydride-ion was attached to the C-1 positions of **4** (and **6**), selectively; (v) the recrystallization of **6** from a mixed solvent of acetonitrile and diethyl ether (1:5, v/v) (several times) provided pure **6** as stable single crystals suitable for the X-ray crystallographic analysis; and (vi) along with the resonance formation of **6** in an organic solvent (e.g., CH_3CN), the crystal structure of **6** also suggested that the formation of a delocalized π-electron system between the 3-guaiazulenyl group and the (2*E*)-3-phenyl-2-propen-1-ylium-ion part was possible.

4. Experimental

4.1. General

Thermal (TGA/DTA) and elemental analyses were taken on a Shimadzu DTG-50H thermal analyzer and a Yanaco MT-3 CHN corder, respectively. FABMS spectra were taken on a JEOL The Tandem Mstation JMS-700 TKM data system. UV–vis and IR spectra were taken on a Beckman DU640 spectrophotometer and a Shimadzu FTIR-4200 Grating spectrometer, respectively. NMR spectra were recorded with a JEOL GX-500 (500 MHz for ^1H and 125 MHz for ^{13}C) or JNM-ECA700 (700 MHz for ^1H and 176 MHz for ^{13}C) cryospectrometer at 25 °C. The ^1H NMR spectra were assigned using the computer-assisted simulation analysis (the software: gNMR developed by Adept Scientific plc) on a DELL Dimension XPS T500 personal computer with a Pentium III processor. Cyclic and differential pulse voltammograms were measured by an ALS Model 600 electrochemical analyzer.

4.1.1. Preparation and spectroscopic properties of (2*E*,4*E*,6*E*,8*E*)-1-azulenyl-3,7-dimethyl-9-(2,6,6-trimethyl-1-cyclohexen-1-yl)-2,4,6,8-nonatetraen-1-ylium hexafluorophosphate (3). To a solution of azulene (**1**) (60 mg, 0.47 mmol) in diethyl ether (1.0 mL) was added a solution of all-*trans*-retinal (160 mg, 0.56 mmol) in diethyl ether (2.0 mL) containing hexafluorophosphoric acid (60% aqueous solution, 0.1 mL). The mixture was stirred at −10 °C for 1 h in a dark room, giving a dark-blue precipitate, which was centrifuged at 2.5 krpm for 1 min. The crude product thus obtained was carefully washed with diethyl ether and dried well in a vacuum desiccator to provide pure **3** as a dark-blue powder (188 mg, 74% yield).

4.1.1.1. Compound 3. Dark-blue powder, mp >135 °C [decomp., determined by thermal analyses (TGA and DTA)]. Found: C, 66.67; H, 6.53%. Calcd for $C_{30}H_{35}F_6P$: C, 66.66; H, 6.53%. UV–vis λ_{max} (CH_3CN) nm (log ε): 683 (4.79). IR ν_{max} (KBr, cm^{-1}): 841 and 559 (PF_6^-). exact FABMS (3-nitrobenzyl alcohol matrix), found: *m*/*z* 395.2724; calcd for $C_{30}H_{35}$: $[M-PF_6]^+$, *m*/*z* 395.2739. ^1H NMR (700 MHz, CD_3CN), signals based on the azulenyl group: δ 7.66 (1H, d, J=4.8 Hz, H-3′), 8.12 (1H, dd, J=9.6, 9.6 Hz, H-5′), 8.19 (1H, dd, J=9.6, 9.6 Hz, H-7′), 8.28 (1H, dd, J=9.6, 9.6 Hz, H-6′), 8.30 (1H, d, J=4.8 Hz, H-2′), 8.65 (1H, d, J=9.6 Hz, H-4′), and 9.12 (1H, d, J=9.6 Hz, H-8′); signals based on the (2*E*,4*E*,6*E*,8*E*)-3,7-dimethyl-9-(2,6,6-trimethyl-1-cyclohexen-1-yl)-2,4,6,8-nonatetraen-1-ylium-ion part: δ 1.09 (6H, s, *gem*-Me_2-6″), 1.507 (1H, dd, J=6.0, 3.2 Hz, Ha-5″), 1.512 (1H, dd, J=6.0, 3.2 Hz, Hb-5″), 1.63 (1H, dddd, J=6.0, 6.0, 6.0, 6.0 Hz, Ha-4″), 1.63 (1H, dddd, J=6.0, 6.0, 3.2, 3.2 Hz, Hb-4″), 1.78 (3H, s, Me-2″), 2.10 (2H, dd, J=6.0, 6.0 Hz, CH_2-3″), 2.12 (3H, s, Me-7), 2.45 (3H, s, Me-3), 6.38 (1H, d, J=16.0 Hz, H-8), 6.42 (1H, d, J=11.6 Hz, H-6), 6.70 (1H, d, J=14.0 Hz, H-4), 6.71 (1H, d, J=16.0 Hz, H-9), 7.38 (1H, d, J=13.2 Hz, H-2), 7.60 (1H, dd, J=14.0, 11.6 Hz, H-5), and 8.56 (1H, d, J=13.2 Hz, HC^+-1). ^{13}C NMR (176 MHz, CD_3CN): δ 167.3 (C-3), 157.5 (C-8a′), 151.8 (C-3a′), 151.4 (C-7), 146.3 (C-6′), 146.1 (HC^+-1), 143.0 (C-4′), 142.8 (C-5), 141.3 (C-5′), 140.0 (C-2′,8′), 139.6 (C-7′), 138.9 (C-1″), 137.7 (C-4,8), 136.4 (C-1′), 135.6 (C-9), 135.3 (C-2″), 132.8 (C-6), 132.6 (C-3′), 131.7 (C-2), 40.7 (C-5″), 35.1 (C-6″), 34.3 (C-3″), 29.4 (*gem*-Me_2-6″), 22.3 (Me-2″), 19.8 (C-4″), 14.9 (Me-3), and 13.7 (Me-7).

4.1.2. Reduction of (2*E*,4*E*,6*E*,8*E*)-1-(3-guaiazulenyl)-3,7-dimethyl-9-(2,6,6-trimethyl-1-cyclohexen-1-yl)-2,4,6,8-nonatetraen-1-ylium hexafluorophosphate (4) with $NaBH_4$. To a solution of $NaBH_4$ (2 mg, 53 μmol) in

methylene-d_2 chloride (1.0 mL) was added a solution of **4** (20 mg, 33 μmol) in methylene-d_2 chloride (1.0 mL). The mixture was stirred at −10 °C for 20 min in a dark room, giving (2*E*,4*E*,6*E*,8*E*)-1-(3-guaiazulenyl)-3,7-dimethyl-9-(2,6,6-trimethyl-1-cyclohexen-1-yl)-2,4,6,8-nonatetraene (**7**), quantitatively, and then filtered. The filtrate was analyzed by the use of exact EIMS and ^{1}H and ^{13}C NMR including 2D NMR (i.e., H–H COSY, HMQC, and HMBC).

4.1.2.1. Compound 7. Green paste [R_f=0.70 on silica-gel TLC (hexane–AcOEt=8:2, v/v)]. exact EIMS (70 eV), found: *m*/*z* 466.3618; calcd for $C_{35}H_{46}$: M^+, *m*/*z* 466.3600. ^{1}H NMR (500 MHz, CD_2Cl_2), signals based on the 3,8-dimethyl-5-isopropylazulen-1-yl group: δ 1.30 (6H, d, *J*=6.9 Hz, $(CH_3)_2$CH-5′), 2.55 (3H, s, Me-3′), 2.91 (3H, s, Me-8′), 3.01 (1H, sept, *J*=6.9 Hz, Me_2CH-5′), 6.83 (1H, d, *J*=10.7 Hz, H-7′), 7.30 (1H, dd, *J*=10.7, 2.2 Hz, H-6′), 7.42 (1H, s, H-2′), and 8.06 (1H, d, *J*=2.2 Hz, H-4′); signals based on the (2*E*,4*E*,6*E*,8*E*)-3,7-dimethyl-9-(2,6,6-trimethyl-1-cyclohexen-1-yl)-2,4,6,8-nonatetraen-1-yl part: δ 1.00 (6H, s, *gem*-Me_2-6″), 1.45 (1H, dd, *J*=6.0, 3.0 Hz, Ha-5″), 1.46 (1H, dd, *J*=6.0, 3.0 Hz, Hb-5″), 1.60 (1H, dddd, *J*=6.0, 6.0, 6.0, 6.0 Hz, Ha-4″), 1.60 (1H, dddd, *J*=6.0, 6.0, 3.0, 3.0 Hz, Hb-4″), 1.67 (3H, dd, *J*=0.8, 0.8 Hz, Me-2″), 1.93 (6H, s, Me-3,7), 2.00 (2H, br ddd, *J*=6.0, 6.0 Hz, CH_2-3″), 4.08 (2H, d, *J*=7.0 Hz, CH_2-1), 5.71 (1H, br t, *J*=7.0 Hz, H-2), 6.086 (1H, d, *J*=16.0 Hz, H-8), 6.089 (1H, br d, *J*=11.2 Hz, H-6), 6.16 (1H, br d, *J*=16.0 Hz, H-9), 6.30 (1H, d, *J*=15.1 Hz, H-4), and 6.60 (1H, dd, *J*=15.1, 11.2 Hz, H-5). ^{13}C NMR (125 MHz, CD_2Cl_2): δ 146.4 (C-8′), 140.7 (C-2′), 139.9 (C-5′), 138.8 (C-1″), 138.73 (C-3a′), 138.71 (C-8), 138.5 (C-4), 135.9 (C-7), 135.7 (C-6′), 135.1 (C-2), 134.4 (C-3), 134.2 (C-4′), 133.4 (C-8a′), 131.7 (C-6), 129.9 (C-2″), 127.5 (C-1′), 127.0 (C-9), 126.9 (C-7′), 125.1 (C-3′), 124.4 (C-5), 40.4 (C-5″), 38.3 (Me_2CH-5′), 34.9 (C-6″), 33.6 (C-3″), 31.4 (C-1), 29.3 (*gem*-Me_2-6″), 27.0 (Me-8′), 24.7 ($(CH_3)_2$CH-5′), 21.9 (Me-2″), 20.0 (C-4″), 12.9 (Me-3,7), and 12.8 (Me-3′).

4.1.3. Preparation and spectroscopic properties of (2*E*)-1-azulenyl-3-phenyl-2-propen-1-ylium hexafluorophosphate (5). To a solution of azulene (**1**) (50 mg, 0.39 mmol) in diethyl ether (0.5 mL) was added a solution of *trans*-cinnamaldehyde (50 mg, 0.38 mmol) in diethyl ether (3.0 mL) containing hexafluorophosphoric acid (60% aqueous solution, 0.1 mL). The mixture was stirred at 25 °C for 1 h, giving a dark-red precipitate, which was centrifuged at 2.5 krpm for 1 min. The crude product thus obtained was carefully washed with diethyl ether and dried well in a vacuum desiccator to provide pure **5** as a dark-red powder (133 mg, 90% yield).

4.1.3.1. Compound 5. Dark-red powder, mp >120 °C [decomp., determined by thermal analyses (TGA and DTA)]. UV–vis λ_{max} (CH_3CN) nm (log ε): 292 (4.07), 319 (4.10), 329 (4.12), and 500 (4.55). IR ν_{max} (KBr, cm^{-1}): 837 and 556 (PF_6^-). exact FABMS (3-nitrobenzyl alcohol matrix), found: *m*/*z* 243.1173; calcd for $C_{19}H_{15}$: $[M-PF_6]^+$, *m*/*z* 243.1174. ^{1}H NMR (500 MHz, CD_3CN), signals based on the azulenyl group: δ 7.82 (1H, d, *J*=5.4 Hz, H-3′), 8.50 (1H, d, *J*=5.4 Hz, H-2′), 8.51 (1H, dd, *J*=10.9, 9.5 Hz, H-5′), 8.55 (1H, dd, *J*=11.2, 10.4 Hz, H-7′), 8.57 (1H, dd, *J*=10.9, 10.4 Hz, H-6′), 8.90 (1H, d, *J*=9.5 Hz, H-4′), and 9.25 (1H, d, *J*=11.2 Hz, H-8′); signals based on the (2*E*)-3-phenyl-2-propen-1-ylium-ion part: δ 7.50 (2H, dd, *J*=8.6, 7.3 Hz, H-3″,5″), 7.53 (1H, dddd, *J*=7.3, 7.3, 1.5, 1.5 Hz, H-4″), 7.83 (1H, d, *J*=15.0 Hz, H-3), 7.83 (2H, dd, *J*=8.6, 1.5 Hz, H-2″,6″), 8.08 (1H, dd, *J*=15.0, 11.7 Hz, H-2), and 8.58 (1H, d, *J*=11.7 Hz, HC^+-1). ^{13}C NMR (125 MHz, CD_3CN): δ 161.4 (C-8a′), 156.7 (C-3), 154.6 (C-3a′), 152.1 (HC^+-1), 147.8 (C-6′), 145.7 (C-5′), 144.3 (C-4′), 143.7 (C-7′), 141.5 (C-2′), 141.0 (C-8′), 139.0 (C-1′), 136.4 (C-1″), 135.4 (C-3′), 133.8 (C-4″), 130.9 (C-2″,6″), 130.4 (C-3″,5″), and 127.4 (C-2).

4.1.4. Preparation and spectroscopic properties of (2*E*)-1-(3-guaiazulenyl)-3-phenyl-2-propen-1-ylium hexafluorophosphate (6). To a solution of guaiazulene (**2**) (100 mg, 0.50 mmol) in acetonitrile (0.5 mL) was added a solution of *trans*-cinnamaldehyde (60 mg, 0.45 mmol) in diethyl ether (5.0 mL) containing hexafluorophosphoric acid (60% aqueous solution, 0.2 mL). The mixture was stirred at 25 °C for 1 h, giving a dark-red precipitate, which was centrifuged at 2.5 krpm for 1 min. The crude product thus obtained was carefully washed with diethyl ether and dried well in a vacuum desiccator to provide pure **6** as a dark-red powder (199 mg, 96% yield). The product **6** was recrystallized from acetonitrile–diethyl ether (1:5, v/v) (several times) to provide **6** as stable single crystals.

4.1.4.1. Compound 6. Dark-red blocks, mp >151 °C [decomp., determined by thermal analyses (TGA[38] and DTA)]. Found: C, 62.82; H, 5.55%. Calcd for $C_{24}H_{25.25}F_6O_{0.125}P$ ($C_{24}H_{25}F_6P$+1/8H_2O): C, 62.57; H, 5.52%. UV–vis λ_{max} (CH_3CN) nm (log ε): 237 (4.38), 294 (4.10), 338 (4.16), and 504 (4.54); IR ν_{max} (KBr, cm^{-1}): 837 and 559 (PF_6^-). exact FABMS (3-nitrobenzyl alcohol matrix), found: *m*/*z* 313.1946; calcd for $C_{24}H_{25}$: $[M-PF_6]^+$, *m*/*z* 313.1956. ^{1}H NMR (500 MHz, CD_3CN), signals based on the 3,8-dimethyl-5-isopropylazulen-1-yl group: δ 1.44 (6H, d, *J*=6.9 Hz, $(CH_3)_2$CH-5′), 2.52 (3H, s, Me-3′), 3.28 (3H, s, Me-8′), 3.44 (1H, sept, *J*=6.9 Hz, Me_2CH-5′), 8.19 (1H, s, H-2′), 8.32 (1H, dd, *J*=11.2, 2.0 Hz, H-6′), 8.37 (1H, d, *J*=11.2 Hz, H-7′), and 8.51 (1H, d, *J*=2.0 Hz, H-4′); signals based on the (2*E*)-3-phenyl-2-propen-1-ylium-ion part: δ 7.42 (2H, dd, *J*=8.3, 6.2 Hz, H-3″,5″), 7.43 (1H, dddd, *J*=6.2, 6.2, 2.0, 2.0 Hz, H-4″), 7.65 (1H, d, *J*=14.9 Hz, H-3), 7.72 (2H, dd, *J*=8.3, 2.0 Hz, H-2″,6″), 7.87 (1H, dd, *J*=14.9, 11.6 Hz, H-2), and 8.45 (1H, d, *J*=11.6 Hz, HC^+-1). ^{13}C NMR (125 MHz, CD_3CN): δ 169.6 (C-5′), 160.7 (C-3a′), 157.2 (C-8′), 152.9 (C-3), 152.1 (C-8a′) 150.8 (HC^+-1), 149.5 (C-7′), 144.5 (C-6′), 143.7 (C-3′), 139.7 (C-2′), 139.7 (C-4′), 136.7 (C-1′), 136.7 (C-1″), 132.7 (C-4″), 130.2 (C-3″,5″), 130.1 (C-2″,6″), 127.6 (C-2), 40.1 (Me_2CH-5′), 29.4 (Me-8′), 23.8 ($(CH_3)_2$CH-5′), and 13.9 (Me-3′).

4.1.5. Reduction of (2*E*)-1-(3-guaiazulenyl)-3-phenyl-2-propen-1-ylium hexafluorophosphate (6) with $NaBH_4$. To a solution of $NaBH_4$ (2 mg, 53 μmol) in methylene-d_2 chloride (1.0 mL) was added a solution of **6** (20 mg, 44 μmol) in methylene-d_2 chloride (1.0 mL). The mixture was stirred at 25 °C for 20 min, giving (2*E*)-1-(3-guaiazulenyl)-3-phenyl-2-propene (**10**), quantitatively, and then filtered. The filtrate was analyzed by the use of exact EIMS

and ^{1}H and ^{13}C NMR including 2D NMR (i.e., H–H COSY, HMQC, and HMBC).

4.1.5.1. Compound 10. Blue paste [R_f=0.61 on silica-gel TLC (hexane–AcOEt=8:2, v/v)]. exact EIMS (70 eV), found: *m/z* 314.2033; calcd for $C_{24}H_{26}$: M^+, *m/z* 314.2035. ^{1}H NMR (500 MHz, CD_2Cl_2), signals based on the 3,8-dimethyl-5-isopropylazulen-1-yl group: δ 1.31 (6H, d, J=6.9 Hz, $(CH_3)_2$CH-5′), 2.58 (3H, s, Me-3′), 2.94 (3H, s, Me-8′), 3.03 (1H, sept, J=6.9 Hz, Me_2CH-5′), 6.85 (1H, d, J=10.9 Hz, H-7′), 7.31 (1H, dd, J=10.9, 2.0 Hz, H-6′), 7.48 (1H, s, H-2′), and 8.09 (1H, d, J=2.0 Hz, H-4′); signals based on the (2*E*)-3-phenyl-2-propen-1-yl part: δ 4.10 (2H, dd, J=6.0, 1.7 Hz, CH_2-1), 6.18 (1H, dt, J=15.8, 1.7 Hz, H-3), 6.57 (1H, dt, J=15.8, 6.0 Hz, H-2), 7.17 (1H, dddd, J=7.3, 7.3, 1.3, 1.3 Hz, H-4″), 7.25 (2H, dd, J=7.6, 7.3 Hz, H-3″,5″), and 7.30 (2H, dd, J=7.6, 1.3 Hz, H-2″,6″). ^{13}C NMR (125 MHz, CD_2Cl_2): δ 146.4 (C-8′), 141.2 (C-2′), 140.0 (C-5′), 138.9 (C-1″), 138.7 (C-3a′) 135.7 (C-6′), 134.2 (C-4′), 133.6 (C-8a′), 133.0 (C-2), 130.9 (C-3), 129.5 (C-3″,5″), 127.9 (C-4″), 127.0 (C-7′), 126.9 (C-2″,6″), 126.4 (C-1′), 125.3 (C-3′), 38.3 (Me_2CH-5′), 35.2 (C-1), 26.8 (Me-8′), 24.7 ($(CH_3)_2$CH-5′), and 12.9 (Me-3′).

4.1.6. X-ray crystal structure of (2*E*)-1-(3-guaiazulenyl)-3-phenyl-2-propen-1-ylium hexafluorophosphate (6). A total of 11,875 reflections with $2\theta_{max}$=54.9° were collected on a Rigaku RAXIS-RAPID Imaging Plate diffractometer with graphite monochromated Mo Kα radiation (λ= 0.71075 Å, voltage=60 kV, current=90 mA) at 93 K. The structure was solved by direct methods (QTAN) and expanded using Fourier techniques (DIRDIF-94). The non-hydrogen atoms were refined anisotropically. The final cycle of full-matrix least-squares refinement was based on F^2. All calculations were performed using the teXsan crystallographic software package. Crystallographic data have been deposited at the CCDC, 12 Union Road, Cambridge CB2 1EZ, UK and copies can be obtained on request, free of charge, by quoting the publication citation and the deposition number CCDC 265281.

Crystallographic data for **6**:[38] $C_{24}H_{18.25}F_6O_{0.13}P$ (FW= 453.70), red block (the crystal size, 0.10×0.10× 0.10 mm^3), monoclinic, *C*2/m (#12), a=17.393(9) Å, b= 6.777(2) Å, c=20.812(8) Å, β=99.84(2)°, V=2417(1) $Å^3$, Z=4, D_{calcd}=1.247 g/cm^3, μ(Mo Kα)=1.67 cm^{-1}, measured reflections=11,875, observed reflections=2984, no. of parameters=211, $R1$=0.080, $wR2$=0.241, and goodness of fit indicator=1.06.

Acknowledgements

This work was partially supported by a Grant-Aid for Scientific Research from the Ministry of Education, Culture, Sports, Science and Technology, Japan.

References and notes

1. Oda, M.; Uchiyama, T.; Kajioka, T.; Hashimoto, T.; Miyatake, R.; Kuroda, S. *Heterocycles* **2000**, *53*, 2071–2077.
2. Oda, M.; Fukuta, A.; Kajioka, T.; Uchiyama, T.; Kainuma, H.; Miyatake, R.; Kuroda, S. *Tetrahedron* **2000**, *56*, 9917–9925.
3. Oda, M.; Fukuta, A.; Uchiyama, T.; Kajioka, T.; Kuroda, S. *Recent Res. Dev. Org. Chem.* **2002**, *6*, 543–563.
4. Okazaki, T.; Laali, K. K. *Org. Biomol. Chem.* **2003**, *1*, 3078–3093.
5. (a) Reid, D. H.; Stafford, W. H.; Stafford, W. L.; McLennan, G.; Voigt, A. *J. Chem. Soc.* **1958**, 1110–1117; (b) Kirby, E. C.; Reid, D. H. *J. Chem. Soc.* **1960**, 494–501.
6. (a) Fraser, M.; Raid, D. H. *J. Chem. Soc.* **1963**, 1421–1429; (b) Hünig, S.; Scheutzow, D.; Friedrich, H. J. *Angew. Chem.* **1964**, *76*, 818.
7. (a) Hünig, S.; Ort, B. *Liebigs Ann. Chem.* **1984**, 1905–1935; (b) Hünig, S.; Ort, B. *Liebigs Ann. Chem.* **1984**, 1936–1951; (c) Hünig, S.; Ort, B. *Liebigs Ann. Chem.* **1984**, 1959–1971.
8. Ito, S.; Fujita, M.; Morita, N.; Asao, T. *Bull. Chem. Soc. Jpn.* **2000**, *73*, 721–727.
9. Ito, S.; Morita, N.; Asao, T. *Bull. Chem. Soc. Jpn.* **2000**, *73*, 1865–1874.
10. Ito, S.; Kikuchi, S.; Okujima, T.; Morita, N.; Asao, T. *J. Org. Chem.* **2001**, *66*, 2470–2479.
11. Ito, S.; Kubo, T.; Morita, N.; Ikoma, T.; Tero-Kubota, S.; Tajiri, A. *J. Org. Chem.* **2003**, *68*, 9753–9762.
12. Ito, S.; Kubo, T.; Kondo, M.; Kabuto, C.; Morita, N.; Asao, T.; Fujimori, K.; Watanabe, M.; Harada, N.; Yasunami, M. *Org. Biomol. Chem.* **2003**, *1*, 2572–2580.
13. Ito, S.; Kawakami, J.; Tajiri, A.; Ryuzaki, D.; Morita, N.; Asao, T.; Watanabe, M.; Harada, N. *Bull. Chem. Soc. Jpn.* **2005**, *78*, 2051–2065.
14. Naya, S.; Nitta, M. *J. Chem. Soc., Perkin Trans. 2* **2001**, 275–281.
15. Cristian, L.; Sasaki, I.; Lacroix, P. G.; Donnadieu, B.; Asselberghs, I.; Clays, K.; Razus, A. C. *Chem. Mater.* **2004**, *16*, 3543–3551.
16. Muthyala, R. S.; Alam, M.; Liu, R. S. H. *Tetrahedron Lett.* **1998**, *39*, 5–8.
17. Asato, A. E.; Li, X.-Y.; Mead, D.; Patterson, G. M. L.; Liu, R. S. H. *J. Am. Chem. Soc.* **1990**, *112*, 7398–7399.
18. Muthyala, R.; Watanabe, D.; Asato, A. E.; Liu, R. S. H. *Photochem. Photobiol.* **2001**, *74*, 837–845.
19. Takekuma, S.; Sasaki, M.; Takekuma, H.; Yamamoto, H. *Chem. Lett.* **1999**, 999–1000.
20. Takekuma, S.; Takata, S.; Sasaki, M.; Takekuma, H. *Tetrahedron Lett.* **2001**, *42*, 5921–5924.
21. Takekuma, S.; Tanizawa, M.; Sasaki, M.; Matsumoto, T.; Takekuma, H. *Tetrahedron Lett.* **2002**, *43*, 2073–2078.
22. Sasaki, M.; Nakamura, M.; Hannita, G.; Takekuma, H.; Minematsu, T.; Yoshihara, M.; Takekuma, S. *Tetrahedron Lett.* **2003**, *44*, 275–279.
23. Sasaki, M.; Nakamura, M.; Uriu, T.; Takekuma, H.; Minematsu, T.; Yoshihara, M.; Takekuma, S. *Tetrahedron* **2003**, *59*, 505–516.
24. Nakamura, M.; Sasaki, M.; Takekuma, H.; Minematsu, T.; Takekuma, S. *Bull. Chem. Soc. Jpn.* **2003**, *76*, 2051–2052.
25. Takekuma, S.; Sasaki, K.; Nakatsuji, M.; Sasaki, M.; Minematsu, T.; Takekuma, H. *Bull. Chem. Soc. Jpn.* **2004**, *77*, 379–380.
26. Nakatsuji, M.; Hata, Y.; Fujihara, T.; Yamamoto, K.; Sasaki, M.; Takekuma, H.; Yoshihara, M.; Minematsu, T.; Takekuma, S. *Tetrahedron* **2004**, *60*, 5983–6000.
27. Takekuma, S.; Hata, Y.; Nishimoto, T.; Nomura, E.; Sasaki, M.; Minematsu, T.; Takekuma, H. *Tetrahedron* **2005**, *61*, 6892–6907.

28. Takekuma, S.; Takahashi, K.; Sakaguchi, A.; Shibata, Y.; Sasaki, M.; Minematsu, T.; Takekuma, H. *Tetrahedron* **2005**, *61*, 10349–10362.
29. Takekuma, S.; Takahashi, K.; Sakaguchi, A.; Sasaki, M.; Minematsu, T.; Takekuma, H. *Tetrahedron* **2006**, *62*, 1520–1526.
30. Takekuma, S.; Hirosawa, M.; Morishita, S.; Sasaki, M.; Minematsu, T.; Takekuma, H. *Tetrahedron* **2006**, *62*, 3732–3738.
31. Takekuma, S.; Sonoda, K.; Fukuhara, C.; Minematsu, T. *Tetrahedron* **2007**, *63*, 2472–2481.
32. Takekuma, S.; Tone, K.; Sasaki, M.; Minematsu, T.; Takekuma, H. *Tetrahedron* **2007**, *63*, 2490–2502.
33. Matsubara, Y.; Yamamoto, H.; Nozoe, T. *Stereoselective Synthesis (Part I)*; Atta-ur-Rahman, Ed.; Studies in Natural Products Chemistry; Elsevier: Amsterdam, 1994; Vol. 14, pp 313–354.
34. Katagiri, K.; Oguchi, Y.; Takasu, Y. *Nippon Kagaku Kaishi* **1986**, 387–392.
35. The reaction of **1** with all-*trans*-retinal in methanol (or diethyl ether) in the presence of hexafluorophosphoric acid at −10 °C for 1 h in a dark room gave the same result.
36. Azulene (**1**). UV–vis λ_{max} (CH_3CN) nm (log ε): 235 (4.23), 270sh (4.70), 273 (4.71), 278 (4.66), 293sh (3.54), 324 (3.49), 338 (3.63), 350 (2.82), 576 (2.53), 622sh (2.45), and 683sh (2.02).
37. Compound **8**: −7.66 eV (π-HOMO); −0.99 eV (π-LUMO); the final value for the gradient norm of the optimized structure **8** showed 0.018. Compound **9**: −7.53 eV (π-HOMO); −0.88 eV (π-LUMO); the final value for the gradient norm of the optimized structure **9** showed 0.010. The following MO calculation program and calculation conditions were used for **8** and **9** (i.e., the software: WinMOPAC Ver. 3.0 developed by Fujitsu Ltd., Japan; semiempirical Hamiltonian: AM1; and keywords: PRECISE, VECTORS, ALLVEC, BONDS, GEO-OK, EF, PL, LET, T=10D, GNORM=10^{-4} and SCFCRT=10^{-10}).
38. The TGA trace of the single crystals of **6** ($C_{24}H_{25}F_6P$+1/8H_2O) displayed a small mass loss between 125 and 130 °C of 0.5% that corresponded to surface dehydration and loss of the extra-framework water molecule (calculated 0.5%).
39. Guaizulene (**2**). UV–vis λ_{max} (CH_3CN) nm (log ε): 213 (4.10), 244 (4.39), 284 (4.61), 301sh (4.03), 348 (3.65), 365 (3.46), 600 (2.68), 648sh (2.61), and 721sh (2.20).
40. Details based on ab initio calculations for **3–6** are further currently under intensive investigation.
41. Zeller, K.-P.; *Methoden der Organishen Chemie*, 4th ed.; Georg Thieme: Stuttgart, 1985; Vol. V/2c, p 127.
42. Bouwstra, J. A.; Schouten, A.; Kroon, J. *Acta Crystallogr.* **1984**, *C40*, 428–431.
43. Santarsiero, B. D.; James, M. N. G.; Mahendran, M.; Childs, R. F. *J. Am. Chem. Soc.* **1990**, *112*, 9416–9418.
44. The optimized (2*E*)-1-azulenyl-3-phenyl-2-propen-1-ylium-ion structure for **5** and the optimized (2*E*,4*E*,6*E*,8*E*)-1-azulenyl-3,7-dimethyl-9-(2,6,6-trimethyl-1-cyclohexen-1-yl)-2,4,6,8-nonatetraen-1-ylium-ion and (2*E*,4*E*,6*E*,8*E*)-1-(3-guaiazulenyl)-3,7-dimethyl-9-(2,6,6-trimethyl-1-cyclohexen-1-yl)-2,4,6,8-nonatetraen-1-ylium-ion structures for **3** and **4** calculated by a WinMOPAC (Ver. 3.0) program using PM3 as a semiempirical Hamiltonian, respectively, showed (i) that the molecular structure of **5** assumed similar conformation to that of **6**; (ii) that the conformations of the (2*E*,4*E*,6*E*,8*E*)-3,7-dimethyl-9-(2,6,6-trimethyl-1-cyclohexen-1-yl)-2,4,6,8-nonatetraen-1-ylium-ion parts of both **3** and **4** (see Chart 1) were similar to that of the retinal iminium-ion part of **15**[43] (see Chart 6); and (iii) that both the (2*E*,4*E*,6*E*,8*E*)-1-azulenyl-2,4,6,8-nonatetraen-1-ylium-ion framework of **3** and the (2*E*,4*E*,6*E*,8*E*)-1-(3-guaiazulenyl)-2,4,6,8-nonatetraen-1-ylium-ion framework of **4** were planar. Similarly, as in the previous paper,[32] the following MO calculation program and calculation conditions were used for **3–5** (i.e., the software: WinMOPAC Ver. 3.0 developed by Fujitsu Ltd., Japan; semiempirical Hamiltonian: PM3; and keywords: CHARGE=1, PRECISE, VECTORS, ALLVEC, BONDS, GEO-OK, EF, PL, LET, T=10D, GNORM=10^{-4}, and SCFCRT=10^{-10}).